

THIS DOCUMENT IS PART OF A NEW BOOK, IT IS BROUGHT TO YOU FREELY BY THE OPEN ACCESS JOURNAL MATERIALS AND DEVICES

Publication date: 2021, january 14th

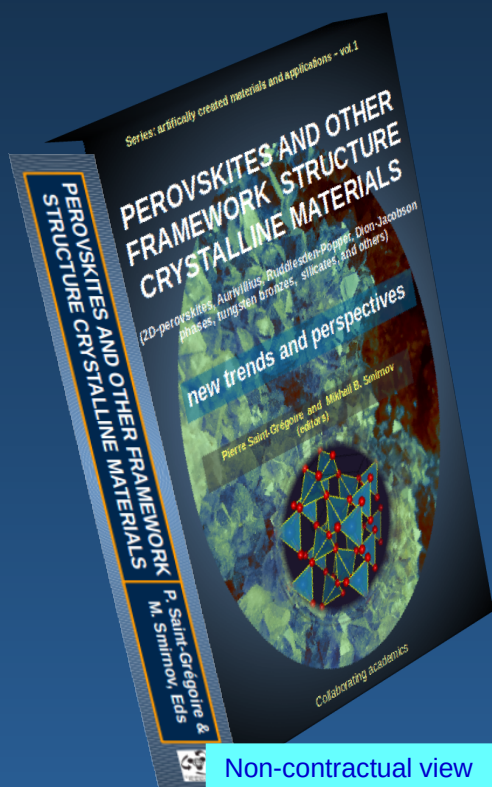
The book,
**“PEROVSKITES AND OTHER FRAMEWORK
STRUCTURE MATERIALS**

(2D-perovskites, Aurivillius, Ruddlesden-Popper, Dion-Jacobson phases, tungsten bronzes, clays, and others)

New trends and perspectives”

(editors P. Saint-Grégoire and M.B Smirnov)

Is a collective volume of 800 pages with **76 authors** and **26 chapters** on recent developments and hot subjects, divided into two parts:



A. Fundamental aspects and general properties

B. Elaborated materials and applied properties

Available in 3 formats:

- Ebook
- printed softcover, black & white
- printed hardcover, color.



Go to the Book(click)

Non-contractual view

Chap. 6 : Properties of $\text{Na}_{0.5}\text{Bi}_{0.5}\text{TiO}_3$ and $\text{Na}_{0.5}\text{Bi}_{0.5}\text{TiO}_3$ -based single crystals

J. Suchanicz (1), K. Kluczevska-Chmielarz (1), P. Czaja (1), M. Nowakowska-Malczyk (2), M. Wąs (2), T. V. Kruzina (3)

(1) Institute of Technology, Pedagogical University, ul. Podchorazych 2, 30-084 Krakow, Poland

(2) Institute of Physics, Pedagogical University, ul. Podchorazych 2, 30-084 Krakow, Poland

(3) Oles Honchar Dnipropetrovsk National University, Prosp. Gagarina 72 49010, Dnipropetrovsk, Ukraine

Corresponding author : jan.suchanicz@up.krakow.pl

Abstract : Most studies of ferroelectric materials were focused on polycrystalline ceramics. However, it is difficult to improve their properties significantly (particularly piezoelectric one) due to grain/grain boundaries, compositional homogeneity, isotropic characteristics, and structural defects. It is commonly accepted that single crystals often have better piezoelectric behavior and less structural defects than ceramics. In this paper, we provide the processing technology and properties of lead-free $\text{Na}_{0.5}\text{Bi}_{0.5}\text{TiO}_3$ and $\text{Na}_{0.5}\text{Bi}_{0.5}\text{TiO}_3$ -based single crystals.

Keywords : FERROELECTRICS, NBT SINGLE CRYSTALS, FLUX METHOD, CZOCHRALSKI METHOD, DIELECTRIC PROPERTIES

Cite this paper: J. Suchanicz, K. Kluczevska-Chmielarz, P. Czaja, M. Nowakowska-Malczyk, M. Wąs, T. V. Kruzina, OAJ materials and Devices, vol 5(1) – chap No6 in “Perovskites and other Framework Structure Crystalline Materials”, p201 (Coll. Acad. 2021) – DOI:10.23647/ca.md20202908

I. Introduction

Polycrystalline ceramics are used in many applications, mainly due to the relative ease of their preparation over an extensive range of compositions and the possibility of obtaining “any” shape and size. However, the presence of grain boundaries, pores and other defects of the crystal structure in polycrystalline, firstly hinders the interpretation of measurement data, and secondly, in many cases, weakens their functional properties. Compared to ceramics, single crystals lead to better chemical homogeneities, control and improved understanding of the crystalline structure. The importance of conducting basic research on single crystals cannot be overestimated also because they are similar to the ideal crystal. Another advantage of single crystals is their transparency, which expands their range of applications. Moreover, the application properties of oriented single crystals with a suitably shaped domain structure significantly outweigh the properties of polycrystalline ceramics. The superior properties of these domain engineered crystals prompted the design of high-performance transducers, sensors, actuators etc. applications ^[1,2].

Quartz and lithium niobate (LiNbO_3) are most known as single crystals. Quartz crystals are widely used for making electrical oscillators and LiNbO_3 crystals are widely used for surface acoustic wave (SAW) devices ^[3]. However, they exhibit inferior piezoelectric performance compared to lead-based crystals. Lead-based crystals includes PMN-PT single crystals (Curie temperature $T_c \approx 130^\circ\text{C}$, above which materials lose their magnetics properties), with piezoelectric parameters that are much higher (so-called "giant" piezo-effect: piezoelectric charge constant $d_{33} > 2000 \text{pC/N}$, electromechanical coupling factor $k_{33} > 90\%$, ($T_c \approx 200^\circ\text{C}$) ^[4, 5]. In order to obtain crystals with a higher Curie temperature, ternary system PIN-PMN-PT ($T_c \approx 200^\circ\text{C}$) were grown. Unfortunately, these single crystals contain toxic lead, which the European Union recommends to eliminate from electronic devices. In addition, both PMN-PT and PIN-PMN-PT single crystals still have non-uniform properties, too high acoustic impedance, which excludes them from many applications, including medicine. The lack of high-quality and large-size single crystals is the biggest hindrance for the advancement of lead-free materials. In addition, due to this, only limited material properties are reported in the literature. Another common problem is the segregation during the growth process, which leads to a local composition gradient along the growth direction.

The most studied lead-free materials are perovskite compounds based on three families: (1) BaTiO_3 (BT), (2) $(\text{Na,K})\text{NbO}_3$ (NKN) and (3) $\text{Na}_{0.5}\text{Bi}_{0.5}\text{TiO}_3$ (NBT). The first family has limited Curie temperature of approximately 100°C , the second one has rather a high Curie temperature (above 300°C). Important lead-free promising material systems are NBT and NBT-based compounds with so called depolarization temperature $T_d \approx 150\text{-}250^\circ\text{C}$ (above this temperature, the material loses piezoelectric

properties). Due to the wide range of properties (piezoelectric, pyroelectric, ferroelectric, etc.) of materials based on NBT and the ease of growing single crystals [e.g. 6-19], technological and research works focus mainly on these materials. In addition, it is very important that the Bi^{3+} ion has similar chemical properties as the Pb^{2+} ion (including high polarization and a tendency to form chemical bonds by hybridization of electronic orbits, which leads to a large distortion of the crystal lattice), whose presence in lead materials promotes their unique properties. In addition, the design materials have been selected so that they contain Morphotropic Phase Boundary (MPB) and phase transformation of the ferroelectric-antiferroelectric type and/or ferroelectric-relaxor type. Near the MPB composition, the coexistence of two different structural phases is relatively less stable, which results in producing larger responses under applied electric field and stress. The presence of the mentioned phase boundary and the mentioned phase transitions favours the induction of extraordinary application parameters. Equally important is the possibility to offer a large range of isovalent substitutes both on the A- and B-site and relatively small degree of Na volatility during growth process of NBT crystals in comparison with NKN. In addition, K_2CO_3 used for NKN obtain is strongly hygroscopic.

Most studies of NBT and NBT-based materials focused on the ceramics since it is difficult to grow high-quality and large-size single crystals mainly due to high volatility of the bismuth and sodium components at melting temperatures.

This work gives a short overview of processing technology and properties of NBT single crystals and its derivatives. The paper does not pretend to fully capture the topic.

II. NBT single crystals growth and properties

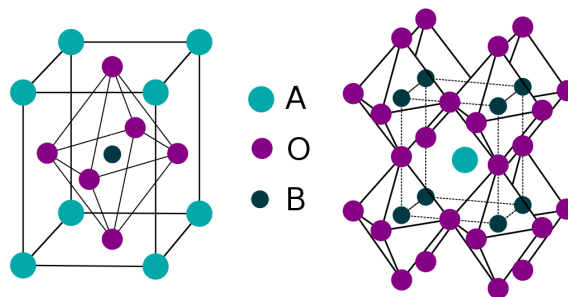


Figure 1: Oxide perovskite structure

II.1 Discovery of NBT and historic overview

NBT was discovered by Smolensky et al. in 1960 ^[20]. At the beginning, this compound did not excite the concern, because exploration was concentrated on lead-based materials. NBT has a perovskite ABO_3 structure (Fig. 1). In 1962, Ivanova et al. ^[21] studied the temperature dependence of crystal structure of NBT in polycrystalline ceramic form. Just in 1974, the next paper on ceramic sample was published, in which the existence of an antiferroelectric state in NBT was postulated ^[22]. However, this hypothesis was not confirmed in any later investigations. In 1979 a paper described optical properties ^[23], in 1980, another paper covered the temperature evolution of thermal expansion ^[24], and in 1982, an article presented the temperature dependence of crystal structure ^[18] and light transmission ^[25] in NBT single crystals obtained by Czochralski method. In 1984 single crystals of NBT were grown by the flux method and their dielectric, pyroelectric and piezoelectric properties were measured ^[26, 27]. The exploration of NBT increased from 1988, when technological conditions and dielectric and electrostrictive properties were described ^[28]. The electric properties of NBT single crystals obtained by the Czochralski method were measured by Kudzin's group from Dnepropetrovsk ^[29, 30]. In 1989 dielectric and pyroelectric behavior of NBT single crystals obtained by improved flux technique were performed ^[31]. Also, in this paper the first signs of time dependence of NBT properties were observed, which were then confirmed in papers ^[15, 32, 33]. The other papers ^[34, 35] contain results of dielectric, optic, pyroelectric, piezoelectric and phase transitions studies of NBT ceramics.

II.2 Dielectric properties of NBT and phase transitions

Figures 2 and 3 show temperature/frequency variation of electric permittivity ϵ of NBT single crystal obtained by flux and Czochralski method, respectively. The local anomaly of ϵ connected with ferroelectric state decay is visible (as rapid increase of ϵ for crystal grown by flux technique). Note the large thermal hysteresis (Fig.3).

The lattice dynamics at phase transitions of NBT single crystals measured by Raman scattering technique were presented by Siny et al. ^[36]. The temperature dependence of the generalized vibrational density of states (VDOS), deduced from inelastic incoherent neutron scattering in the temperature range $-220-30^\circ\text{C}$ of NBT single crystals were presented by Lushnikov et al. ^[37]. The total density of states (DOS) and the projected density of states (PDOS) studying by first-principles the local density calculations were presented by Xu and Ching ^[38]. They only considered the rock salt type of chemical order and did not include any structural relaxation. More accurate first-principles calculations to investigate the electric and optic properties of NBT were performed by Zeng et al. ^[39].

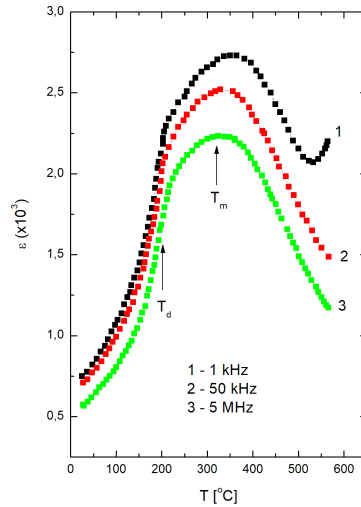


Figure 2: Temperature dependence of the electric permittivity of NBT single crystal obtained by flux method at various frequencies

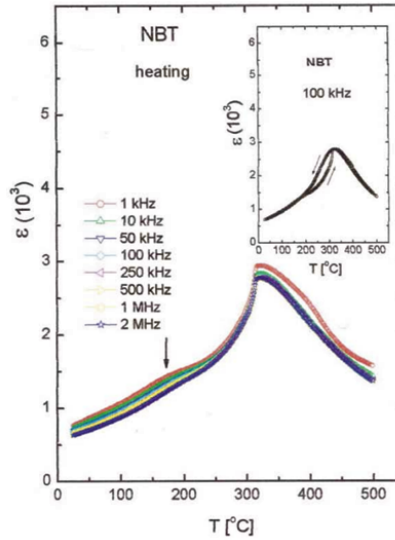


Figure 3: Temperature/frequency dependence of the electric permittivity of NBT single crystals obtained by Czochralski method (on heating)

The arrow indicates the local anomalies (temperature T_d) related to a ferroelectric phase decay. The insert shows the temperature dependence of the electric permittivity of NBT single crystals on heating/cooling showing large thermal hysteresis.

The complex dielectric functions, optical constants such as absorption spectrum, refractive index, extinction coefficient, reflectivity, and energy-loss spectrum were calculated in that paper. It was also concluded that NBT has a direct band gap of 2.1 eV. The comparative studies of crystal structure, domain structure, calorimetric and dielectric properties of two NBT single crystals grown by flux and by the Czochralski methods were presented by Park group [40, 41]. It was found that both crystals show differences in properties under investigations, which can be related to nonstoichiometry induced in crystals grown by Czochralski technique. This nonstoichiometry resulted in less lattice distortion, a lower degree of cation ordering and a larger domain width in twin configuration [41]. The first paper, which contains data of temperature evolution of crystal structure of single crystals obtained by flux method was published in 1995 [6], the next one in 1999 [42].

The research on NBT has accelerated after a European Union directive that appeared in 2002, which recommended replacing in electronic devices the widely used lead-based materials, by lead-free ones. At present, there are in literature several hundred of papers on pure NBT properties.

NBT undergoes the following transformational sequence on cooling: from cubic ($Pm\bar{3}m$) to tetragonal (P4bm or P4/mbm) and finally to rhombohedral/monoclinic (R3c or Cc) with phase transition temperatures of about 540-520 and about 300-260°C, respectively [6, 18-22, 42-45]. Both transitions are not observed as sharp phase transitions but are characterized by a coexistence of cubic/tetragonal and tetragonal/rhombohedral phases in the above temperature intervals, respectively [46]. The large thermal hysteresis of electric permittivity, birefringence, DSC curve, elastic stiffness constant, etc. are observed in the temperature interval of rhombohedral/tetragonal phases coexistence [7, 8, 23, 35, 46].

It was experimentally proved that electric field application improves the polarization/domain ordering, the transformation of tetragonal regions into a rhombohedral phase and supported and extended the ferroelectric phase existence towards higher temperatures [46]. This is accompanied by a change of rhombohedral lattice distortion and a change of unit cell constants. Rhombohedral and tetragonal phases exhibit a ferroelectric and ferroelastic nonpolar (weakly polar) order, respectively. It was shown that at about 280°C the content of rhombohedral phase increases above 80% of the sample volume on cooling [6]. However, transmission electron microscopy (TEM) studies reported an intermediate orthorhombic (Pmn2₁ or Pnma) phase [47]. These investigations showed that the destruction of the rhombohedral phase by microtwinning process of domains starts at about 170°C and that rhombohedral-tetragonal phase transformation at about 279°C can pass through the intermediate orthorhombic phase. The orthorhombic phase develops in the temperature range of ≈170-280°C. Recently, there has been an increase in experimental results showing a departure from pure rhombohedral symmetry. It was

found that the splitting of Bragg peaks existing in-high-resolution reciprocal-space maps suggests lower average structure of NBT than rhombohedral one [48]. Aksel et al. pointed out that the structure is monoclinic (Cc) instead of rhombohedral [49]. High-resolution synchrotron X-ray diffraction study made by Rao et al. revealed a rhombohedral/monoclinic phase coexistence model and it appeared that an electric field induced a monoclinic to rhombohedral phase transformation [50]. A rhombohedral phase with an incommensurate modulation along the four-fold axis of the precursor tetragonal phase was also postulated [51]. In each of these transformations several phases are present simultaneously over a wide temperature interval, making the phase transformation diffuse. Thus, below about 260°C the structure has been reported to be described as rhombohedral, monoclinic or by a coexistence of both depending on thermal, electric and mechanical treatments [52].

II.3 Important characteristic temperatures in NBT

Except temperatures of structural phase transformations, NBT has three characteristic temperatures.

- The first one $T_d \approx 190\text{-}200^\circ\text{C}$, at which the material possesses a long-range ferroelectric state (it is the so called “depolarization temperature) and transforms to a short-range relaxor-like phase. At about this temperature a local anomaly of electric permittivity with a weak relaxor character can be noted.
- The second one, 280°C , is the temperature at which unstable polar regions dynamically existing at higher temperatures, become stable [44]. A sudden increase in the content of the tetragonal phase was observed there, at the expense of the rhombohedral phase and the fastest increase in electrical permittivity during heating, and there was a transition from non-ergodic to ergodic behavior [31, 53]. The existence of unstable polar regions at high temperatures (far above T_m) and their stabilization below 280°C was confirmed by Suchanicz et al. and by Roleder et al. [28, 31]. These polar regions become the nuclei of the low-temperature ferroelectric phase.
- The third one $T_m \approx 320^\circ\text{C}$, at which a diffuse maximum of electric permittivity occurs. This maximum, as for relaxors, does not correspond with any structural phase transition (see for example papers mainly based on neutron scattering measurements described by Vakhrushev group [44, 54-60]). As mentioned above, in high temperatures (far above T_m), unstable polar regions exist, the size of which and correlation radius increase on cooling.

Below the temperature of 420°C there is a wide temperature range in which two

phases, the tetragonal and the rhombohedral phases coexist [6]. In this temperature interval, the content of tetragonal phase decreases at the cost of rhombohedral one on cooling. At about 320°C each phase occupies exactly a half of the sample volume. The maximum of electric permittivity observed at this temperature may be explained as a result of changes in dynamics and size of polar regions and their interaction (both electrical and mechanical) with nonpolar phase (e.g. gradual transition of rhombohedral phase into tetragonal one on heating) [16, 28, 61].

II.4 Coercive field in NBT

NBT exhibits a high coercive field ($E_c \approx 70$ kV/cm), and a considerable remnant polarization ($P_r \approx 35 \mu\text{C}/\text{cm}^2$). Aside from reduced toxicity on processing and use, this material has higher fracture toughness, higher strength and elastic moduli and lower density than the lead-based compounds. However, its electric conductivity is relatively high, which combined with high E_c makes it difficult to pole. To overcome this problem, a new procedure of poling was proposed [62-64], consisting in the simultaneous action of an electric field and perpendicularly to it, a uniaxial pressure.

II.5 Domain structure of NBT

The effects of a uniaxial pressure on optical properties and on domain structure of NBT single crystals were described in [9, 14, 65, 66]. It was shown that it is possible to obtain a stable ferroelastic monodomain state at high temperature under a uniaxial pressure <100 bar. This monodomain state is kept after cooling the sample to room temperature. The controlled modification of domain structure is important, because it greatly affects properties of the material.

II.6 Thermal and dielectric properties of NBT

The first measurements at low-temperature (5-186K) of specific heat (C_{expt}), thermal conductivity (λ), dielectric and pyroelectric properties of NBT single crystals were made by Suchanicz et al. [11, 12]. The broad maximum on $C_{\text{expt}}T^{-3}$ plot in the temperature range $10\text{K} < T < 25\text{K}$ was reported and a rapid rise in this plot with decreasing temperature below $\approx 10\text{K}$ was observed (Fig. 4). This maximum can be represented by a single Einstein mode (51 cm^{-1}), and the fitted Debye temperature (180K) is close to the value obtained from pyroelectric measurements [11]. A similar feature was observed for $(\text{Na}_{0.5}\text{Bi}_{0.5})_{0.86}\text{Ba}_{0.14}\text{TiO}_3$ single crystal [13]. It was shown that a nearly temperature independent regime (plateau) of $\lambda(T)$ and of the electric permittivity $\epsilon(T)$ appears, which corresponds with anomaly in the $C_{\text{expt}}T^{-3}$ curve. As these non-Debye low-

temperature features are observed in monocrystalline as well as in polycrystalline samples they cannot be related to grain boundary mechanisms. In addition, introducing substitutional impurities into the samples has only a small influence on these features. This indicates that this glass-like behaviors are related rather to intrinsic mechanisms and not to impurity doping ^[11, 12].

II.7 Influence of uniaxial pressure on dielectric and ferroelectric properties of NBT single crystals

The first measurements of the influence of a uniaxial pressure on dielectric and ferroelectric properties of NBT single crystals were made by Suchanicz ^[67]. It was found that a uniaxial pressure applied parallel to electric field imposes a significant influence on properties under investigation.

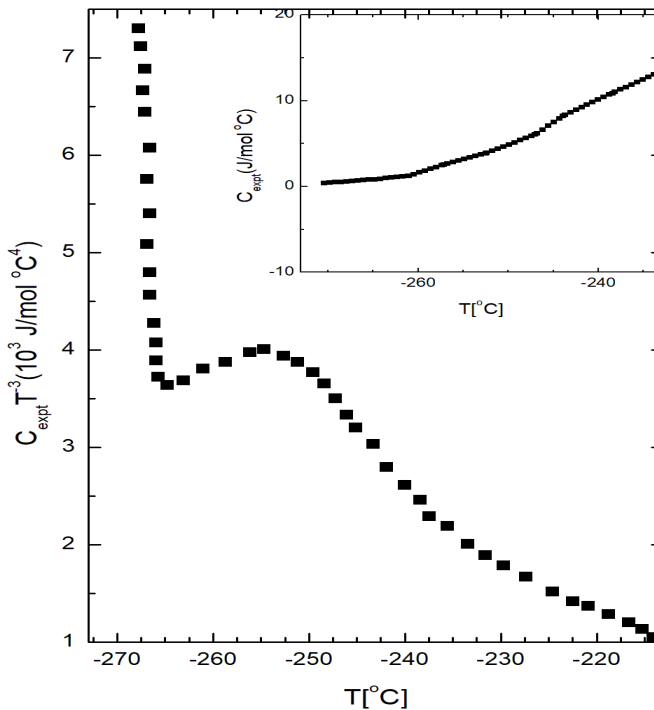


Figure 4: Specific heat of NBT single crystals obtained by flux method plotted as $C_{\text{expt}}T^{-3}$ vs. T

The insert shows the specific heat of NBT single crystals plotted as C_{expt} vs. T in a wide temperature range (based on ^[11]).

This includes: (1) the increase of the rhombohedral-tetragonal phase transition and the decrease of the thermal hysteresis of the permittivity, which can be an evidence of changes of the transition nature to that of the second order one, and (2) the decrease of the polarization in the ferroelectric phase and the broadening of the temperature dependence of the polarization ^[67].

The first elastic constant matrix at room temperature and the temperature dependence of C_{11} constant (30-400°C) of $\text{Na}_{0.5}\text{Bi}_{0.5}\text{TiO}_3$ single crystal were measured by Suchanicz ^[7]. It has been shown, that the difference in the values of the main elastic constants is rather small, mainly due to the slight distortion of the rhombohedral phase. C_{11} constant exhibits anomalies near the temperatures 200 and 320°C that are characteristic for NBT.

It was found that the electrical properties of NBT single crystals were significantly sensitive to thermal treatment (under air or vacuum conditions) ^[68, 69]. It includes a change of impedance and the appearance of a low-frequency relaxation process. It is supposed that slow relaxing dipolar complexes and mobile structural defects are created by oxygen vacancies, which is responsible for this relaxation process.

II.8 Studies of domain structure in NBT single crystals

The first systematic studies of temperature evolution of domain structure (also under uniaxial pressure action) of NBT single crystals were made in 2001 by Kruzina, Duda and Suchanicz ^[9].

It was shown for the first time, that the shape, size and position of ferroelastic domains were unchanged upon cooling from 540°C to room temperature, despite two phase transitions (from cubic to tetragonal, and from tetragonal to rhombohedral one) occur. These results were confirmed and expanded in 2010 by the Viehland group ^[70, 71] for NBT single crystals obtained by top-seeded solution grown technique and in 2017 by Babu et al. ^[72] for single crystals obtained by high-temperature self-flux method.

At 540°C a phase transformation takes place and a twin structure appears, represented by two orientational states separated by coherent (110)-type walls perpendicular to the (001)-plane (Fig. 5) ^[9]. Due to the difference in orientations of domains indicatrix, an optical contrast between adjacent domains occurs. The absence of a noticeable anomaly of electric permittivity near 540°C, the character of domain structure which follows from theoretical group consideration ^[73] and the change of domain structure under uniaxial pressure action may be the reason of the $Pm\bar{3}m \rightarrow 4/mmm$ phase transformation, which is ferroelastic in nature.

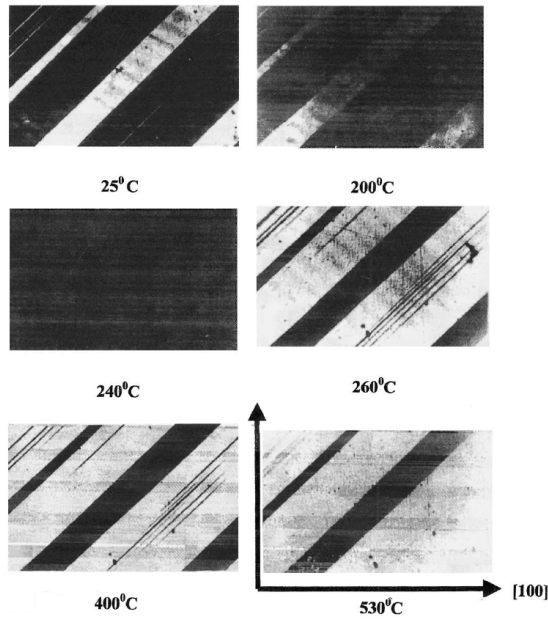


Figure 5: Temperature behavior of the domain structure of NBT single crystals obtained by Czochralski method (based on [9]).

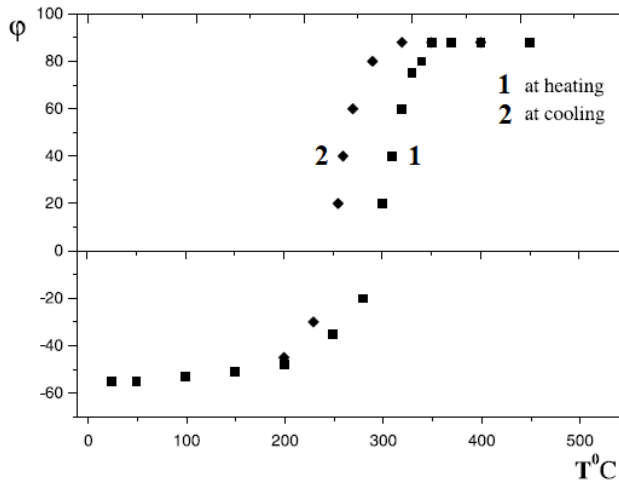


Figure 6: Temperature dependence of extinguishing angle between the indicative states of NBT single crystal obtained by Czochralski technique showing large thermal hysteresis (based on [9]).

The orientation of domain walls practically does not change during cooling to room temperature (Fig. 6). However, starting from about 350°C, changes of the extinction positions with respect of the pseudocubic (100) direction appear in every domain ^[9]. This leads to a decrease of the angle between projections of the slow speed axis of the optical indicatrix in adjacent domains on the (001) plane. At about 240°C the sample looks like an optically isotropic material- it is dark in any position between crossed Nicols and there is no change to distinguish optically the difference between orientational states. However, with a further decrease in temperature, a contrast between the domains reappeared, but now it is opposite to the previous contrast, i.e. precedently light domains look dark and vice versa^[9]. In cooling, changes of indicatrix continue and practically cease at about 150°C (Fig. 7). According to many studies, the R3c polar phase exists at room temperature ^[9, 18, 56], so that extinction positions in each domain do not coincide with the expectation for the rhombohedral phase. The total change of angle φ between neighbouring domains is about $\sim 140^\circ$ (Fig. 7). The temperature dependence of φ (Fig. 7) is correlated with the temperature behaviour of birefringence of single domain crystals ^[35]. In Figure 6, in the illuminated region, it is possible to observe a contrast between domains separated by (100)-type walls, the structure of which differs from the structure of the above discussed (110) walls.

Despite the electrical neutrality of the crystal structure of NBT, there may be some disturbances in the crystal structure due to differences between the states of charge, radii and electron configurations of external shell of Na^+ and Bi^{3+} . It may be supposed that in cubic phase (above about 540°C) these ions are in a disordered arrangement in the A-site ^[9]. Below about 540°C a tetragonal distortion of TiO_6 octahedra takes place and a definite ordering in the arrangement of mentioned ions is expected. Below about 350°C, a rhombohedral distortion of TiO_6 octahedra gradually appears and a new ordering configuration in the arrangement of Na^+ and Bi^{3+} ions should be profitable ^[9]. However, partially frozen A-site still corresponds to the high-temperature tetragonal phase, which leads to the appearance of internal mechanical stress.

Taking into account the thermal changes of the elastic strain tensor components, it may be expected that the angle between indicatrix in two adjacent domains presents a temperature dependence. Indeed, the temperature variations of the elastic constant (C_{11}) of NBT single crystal exhibits an anomalous behaviour in the same temperature interval where the angle φ appears and also shows a remarkable hysteresis ^[7]. On further cooling, the rhombohedral distortion increases, which leads to relaxations of Na^+ and Bi^{3+} ions to configuration in accordance with the rhombohedral phase. Results collected in ^[33] confirm the relaxation process in the temperature interval $\approx 220\text{-}360^\circ\text{C}$. It was shown that at fixed temperatures from this interval, the value of electric permittivity was achieved in time intervals $\approx 40\text{-}50$ min at 360°C and more than 200 min at 270°C. Because the relaxation time strongly increases with decreasing temperature, it is expected that with an insufficiently slow cooling internal mechanical stress may still

remain at room temperature ^[9]. In this case distinguishing position between adjacent domains may differ from that forecast for the rhombohedral phase ^[9]. The internal mechanical stress may be the main reason of large thermal hysteresis of many quantities.

It was found that unique hierarchical domains exist in NBT single crystals ^[70, 71]: (1) a high-temperature tetragonal ferroelectric domain structure is elastically inherited into a lower temperature rhombohedral ferroelectric phase, and (2) polar regions nucleated within this geometrical constraint on cooling. The polar regions seem to have a tendency to align along the (110) and planar defects along these (110) boundaries reduces the elastic energy by partially relaxing the coherence of the lattice.

Babu et al. ^[72] have grown NBT single crystals by high-temperature self-flux method using $25\%\text{Bi}_2\text{O}_3+5\%\text{Na}_2\text{CO}_3$ flux. Initially, they synthesized NBT powder by the solid-state reaction technique, and then this powder was mixed with flux. The crystals growth was performed at 1350°C with 5h soak time and cooled to 1050°C with $3^\circ\text{C}/\text{h}$ cooling rate, after that it was cooled at $200^\circ\text{C}/\text{h}$. As mentioned above, the temperature dependence of domain pattern of obtained NBT crystal is similar to that obtained earlier by Kruzina, Duda and Suchanicz ^[9]. It was shown that with increasing temperature, the birefringence decreases with the disappearance of stripe-like pattern near 225°C ^[72]. However, with further increase of temperature, the stripe-like pattern re-appears above 240°C with a polarization reversal ^[72]. A similar behavior was observed near 205°C on cooling. These results are in concurrence with the dielectric and piezoelectric data ^[72]. It was concluded that this unusual behavior of domains structure was attributed to the ferroelectric-ferroelastic transition ^[72].

The pseudo-dielectric function of NBT single crystals growth by Czochralski technique was obtained in the spectral range of electronic excitations (2-9.5 eV) by spectroscopic ellipsometry using the synchrotron radiation source ^[74]. The spectrum contains two broad absorption bands with maximum at 4.3 and 7.0 eV, which correspond to the inter-band optical transitions from prevalingly 2pO valence bands to the relatively localized 3dTi and 6pBi originated conduction bands. These measurements have shown complicated phase transformations in temperature interval $180\text{-}320^\circ\text{C}$, partially caused by the temperature changes of the domain structure.

The first Raman scattering at normal scattering geometry on single crystals growth by Czochralski method were done in 1986 ^[78], the next in 1991 ^[79] and in 2000 ^[77]. Temperature dependent Raman studies (also high-pressure) of NBT single crystals and ceramics were reported in subsequent papers ^[78-83]. From theoretical and experimental investigations of Raman modes, Born effective charges, phonon frequencies, static dielectric constant tensor components and ionic displacements for all modes were reported ^[79].

II.9 Spectroscopic studies of NBT and Raman scattering results theoretical results

The results from dielectric, Raman, pyroelectric and ferroelectric investigations of Mn and Cr-doped NBT single crystals obtained by Czochralski method were presented by Suchanicz et al. [84]. The influence of this doping on properties measured manifests itself in several ways: (1) an increase of the electric permittivity, (2) an increase of the remnant polarization and the decrease of coercive field, (3) an improvement of pyroelectric properties and (4) an increase of T_m temperature. The results indicate that the substitution of a small amount of foreign ions affected the local crystal structure. No evidence of an antiferroelectric phase was found in NBT-doped single crystals [84].

Theoretical considerations were only scarcely used for studying NBT. Apart from investigations made by Xu and Ching [38] and mentioned above, Burton and Cockayne [85], based on *ab initio* calculations, predicted a monoclinic structure (Pm) within a 40 atoms supercell with “criss-cross” rows of Na and Bi perpendicular to (001). Furthermore Gröting et al. [86], used first-principle calculations based on density functional theory, the influence of chemical order on the thermodynamic stability and local structure were explored. They found out that the hybridization of Bi6sp with O2p-states leads to stereochemically active Bi³⁺ lone pairs and increases the stability of structures with high Bi concentrations in {001}-planes. The same group [87] studied also the kinetics of octahedral tilt transitions by electronic structure calculations within density functional theory. This group showed that the activation energy is lower for structures with 001-order compared to such with 111-order; they deduced also that the deformation energy of the neighbouring octahedra is less in rhombohedral than in tetragonal structure. In subsequent paper [88], the kinetics of phase transitions by octahedral tilts and A-cation displacements by means of density functional theory calculations were examined, by employing *ab initio* molecular dynamics and calculation of nudged elastic band.

It was shown that:

- the energetic differences between rhombohedral, intermediate orthorhombic and other metastable phases are close to the room-temperature thermal energy
- the chemical A-cation order affects energy barriers, influences the coupling between rotational and displacive modes, and determines the stability of certain octahedral tilt orders.

Then, the investigation was performed, using a density functional theory approach, on the ion conductivity versus temperature dependent activation energy of doped or non-stoichiometric NBT [88]. Authors showed that oxygen migration barriers are highly dependent on the local symmetries, the A-cation order, tilt configurations and the different oxygen migration paths, and the phase dependent change of the

migration/association energy are responsible for the change of activation energy of oxygen migration ^[88]. Lü, S.Wang and X.Wang, basing on a [111] ordered structure, studied the structural, electronic and dynamical behaviour of NBT within a density functional formalism ^[89]. The direct band gap was determined to be 2-3eV for rhombohedral, tetragonal and cubic phases. Soft modes were found in both cubic and tetragonal phases. The A modes present vibration of Bi atom in antiphase to other atoms, displacement of Na atom along polar axis rotation and octahedral along the polar axis. The softest E mode presents the movement of Bi atom in the opposite direction to all other atoms. The E mode involves also the largest magnitude of Na displacement, and the other modes are dominated by Ti-O stretching and the vibration of O atom ^[89].

III. Barium titanate BaTiO_3 (BT) and NBT-BT

III.1 Phase transitions in Barium titanate BaTiO_3

Barium titanate BaTiO_3 (BT) has been extensively studied and widely applied because of its proven superior electrical and optical properties ^[90]. From low temperature to high temperature, it undergoes three successive phase transformations: from rhombohedral (R3m) phase to an orthorhombic (Amm2) phase at about -90°C , then to a tetragonal phase (P4mm) at about 5°C and finally to a cubic phase ($Pm\bar{3}m$) at about 120°C . The cubic phase is paraelectric while the other phases are ferroelectric. BT was believed to be a typical displacive-type ferroelectric material, although some experimental results suggest the possibility of formation of pretransitional polar regions in the cubic phase (i.e. an order-disorder mechanism was also postulated). However, the roles and natures of the displacive and order-disorder components during the phase transition are still controversial and remain far from being completely understood.

As mentioned above, NBT single crystals are difficult to pole because they have relatively high both conductivity and coercive field. This causes problems in the polarizing process, and thus leads to low piezoelectric properties. Optimizing processing (for example, using different techniques of single crystal growth) and modifying composition (creating NBT-based solid solutions) are major ways to overcome these problems. Unfortunately, the improvement of piezoelectric and dielectric properties usually leads to the decrease of depolarization temperature T_d . However, high operating temperature interval are needed for many applications. In general, a low T_d value is undesirable in fabricating high-performance NBT-based materials. On the other hand, when T_d is shifted to room temperature, large electric-field-induced strain can appear. Usually, the level of this strain depends on the point

defects concentration level and the aging time. This effect may originate from a defect-mediated reversible domain switching ^[91]. High-strain piezoelectric materials are used in nonlinear actuators and in high-precision positioner devices. The defect types/level will be controlled by the crystal growth conditions, by the donor/acceptor doping and by the annealing process in different atmospheres (air, vacuum, nitrogen etc.) (defect engineering). There is a close relationship between the defects engineering and dielectric, piezoelectric, pyroelectric etc. properties and temperature stability of these properties. In particular, the role of oxygen vacancies in perovskites in the formation of nanopolar regions and coupling between the dipoles and in the formation of the long/short-range ordering is very important.

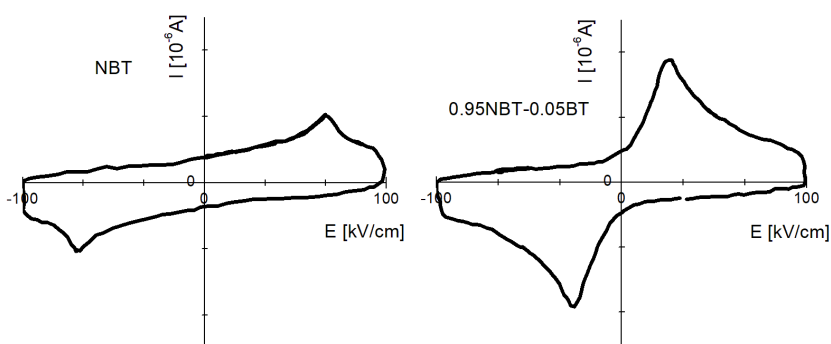


Figure 7: Examples of current hysteresis loops of (1-x)NBT-xBT single crystals (based on ^[8])

III.2 Dielectric properties of NBT-BT single crystals

The first paper on dielectric, piezoelectric and domain structure features of NBT-BT single crystals obtained by Czochralski technique was published by the Kudzin group in 1997 ^[92]. It was shown that these crystals have improved the mentioned properties in comparison to pure NBT. However, in opposite to pure NBT, their monodomain state obtained by the action of a uniaxial pressure at high temperature, is not kept after cooling to room temperature. It was found that the incorporation of Ba²⁺ ions into NBT single crystals leads to improve their dielectric, ferroelectric, pyroelectric and particularly piezoelectric parameters and relaxor behaviour ^[8, 10, 93, 94] (Fig. 7). The broad anomalies observed in temperature evolution of thermal expansion, heat capacity and the transmitted light were associated to structural, dielectric and ferroelectric anomalies, and related to temperature features of polar regions and formation of long-range ferroelectric phase ^[8, 93, 94]. It was postulated that the relaxor behaviour of this system can be related to the local electric and strain fields caused by the

inhomogeneity of the ions distribution and the mismatch in size and charge between Na^+ , Bi^{3+} and Ba^{2+} ions [8, 93, 94].

III.3 Growth of NBT-BT single crystals

The first paper on NBT-BT single crystals growth by flux method and their dielectric, piezoelectric properties was published by Chiang group in 1998 [95], the next ones in 1999 [96] and in 2000 [97]. The properties of these crystals (particularly piezoelectric one) were significantly improved in comparison to pure NBT. NBT-BT single crystals exhibit a strain up to 0.25% with low hysteresis along the cubic (001) direction and strain as high as 0.85% with a greater hysteresis in rhombohedral and tetragonal phase, respectively [95]. However, the crystal structure of this system, particularly at the MPB has remained elusive and no true consensus has been reached regarding the average/local structure-property relationship. The crystal structure, dielectric and ferroelectric properties of NBT-BT single crystals obtained by flux and Bridgman method were presented in paper [98]. The first Raman scattering measurements (isofrequency method) results of (1-x)NBT-xBT (x=0.14) single crystals obtained by Czochralski technique were presented in [99]. The results show that polar region dynamics are accompanied by nonelastic light scattering anomalies.

III.4 NBT-BT samples – influence of doping and growth methods

The peculiarities of phase transformations of (1-x)NBT-xBT (0<x<0.06) single crystals grown by Czochralski method were investigated by means of dielectric and acoustic emission techniques [100]. The results show some differences in temperatures, at which anomalies detected by both techniques appear. It was established that all these temperatures decrease as Ba content increases.

The NBT and NBT-based single crystals were grown by several techniques as flux, high-temperature self-flux, top seeded solution, Czochralski, hydrothermal, Bridgman and modified Bridgman methods.

The growth process and some properties of NBT-BT single crystals were reported in many papers [8, 10, 93, 94, 101-104, 111-121].

Many useful informations about phenomena existing in NBT-BT materials can be found in [105-110].

The Mn-doping of NBT single crystal has resulted in an enhancement of the piezoelectric, ferroelectric and electric (dielectric) properties [122]. It was shown that the Mn substitution in the NBT crystal results in both hardening and softening effects due

to the existence of mixed valence states of Mn ions ^[123].

Also, Mn-doping of NBT-BT single crystals could enhance piezoelectric ($d_{33}=483\text{pC/N}$, $k_t=55.6\%$) and ferroelectric ($P_r=45.3\mu\text{C/cm}^2$, $E_c=2.91\text{kV/cm}$) properties significantly, and can increase structural thermal stability (depolarization temperature T_d) ^[113, 117, 124].

Yao et al. ^[125] reported the following effects with Mn substitution to NBT-BT single crystals: (1) an increase of ferroelectric ordering and in-plane octahedral tilting, (2) formation of structural modulation across domain boundaries, which help relax between domains, and (3) an increase in the number of in-phase oxygen tilted regions with a tendency of alignment along (110). In addition, the tetragonal domain structure could be stabilized by poling along (001) direction and piezoelectric coefficient d_{33} could reach above 500pC/N.

The following effects appear with Ce substitution to NBT-BT single crystals: (1) an increase of depolarization temperature T_d , (2) an increase of the remnant polarization and coercive field and (3) induce relaxor-like behaviour ^[101]. The postulated main reasons behind these effects are the increase of inhomogeneity in A-site ordering and the induction of lattice stresses by the Ce introduction to NBT-BT ^[101].

It is possible to obtain perovskites ABO_3 single crystals by crystallization in liquid phase. However, for majority of these materials this method is not adequate, because they melt incongruently or decompose below melting temperature. It is possible to decrease the crystallization temperature using appropriate solvents (so called flux method). Quantity, size and quality of crystals obtained by this method depend mainly on temperature interval of crystallization and cooling rate. Conditions of stable growth of crystals such as choice of solvent, of furnace material, proportion of starting chemicals, temperature interval of crystallization and rate of temperature change are chosen empirically the most often. Additional difficulties appear in the crystallization of solid solutions crystals. Namely, it happens that the chemical formula of obtained solid solutions crystals may be significantly different from that expected from starting mixtures, and the concentration of particular components may be non-uniform in crystal volume.

For some of the perovskite structure materials, there is an undesirable tendency of pyrochlore phase growth (particularly for Pb-containing ones). The excess of divalent or trivalent component in the flux should improve the crystal growth conditions of the perovskite structure and allow to overcome the pyrochlore tendency. The main advantages of flux method are the decrease of crystallization temperature and the obtention of crystals exhibiting a well-developed crystal habit, which makes the sample orientation easier for studies along selected directions. Sometimes it is the only method to obtain good quality crystals. However, the disadvantages of this method is the relatively small mass of obtained crystals in comparison to mass of starting chemicals and the possibility that ions from the crucible or the solvent enter the crystal

structure. Usually, the size of single crystals obtained by this method remains relatively small. In order to obtain large crystals, other techniques are used, e.g. the modified Bridgman (Zone Melting). In addition, with the use of the modified Bridgman method, only a portion of the ceramic starting material is melted at any time limiting the amount of chemical segregation that takes place along the boule length by preventing convective flow in the melt ^[123]. This results in a more compositionally uniform grown crystal.

III.5 Crystal growth techniques

For the growth of high-quality and large-size perovskite lead-free single crystals (particularly NBT-based ones), the top-seeded solution growth (TSSG) technique is usually used. NBT and NBT-BT crystals growth is generally performed in the following way. High-purity Na_2CO_3 , BaCO_3 , Bi_2O_3 and TiO_2 chemicals are mixed according to stoichiometric ratio and then are heated in a Pt-crucible at 1150-1250°C for 8-10h to form polycrystalline materials. These materials are then mixed with 15-25wt% of excess Bi_2O_3 and Na_2CO_3 as a self-flux. This mixture is thereafter heated to 850-950°C for 1-2h. (001)-oriented NBT and NBT-BT crystal are used as a seed crystal. The soaking in the melt is done at a temperature slightly higher than the melting point for about 5h. Then the temperature is decreased slightly lower than the melting point. When the crystal diameter attains a sufficient value, the crystal starts to pulling up at a rate of 1.5-3 mm/day and rotating at 10-30 rpm. After the crystallization process, the crystal is cooled to room temperature at a rate of 30-50°C/h. Due to a slow solute diffusion process in the TSSG method, the crystal growth speed has to be carefully controlled.

However, if the product is an incongruently melting compound, single crystals have a non-uniform chemical composition and consequently, their properties are not uniform across the sample ^[127]. To overcome this problem, one can use another technique, the solid-state crystal growth (solid-state conversion growth (SSCG)). This technique is similar to the conventional sintering process. In this method, a seed crystal is bonded to the surface of the ceramic compact or embedded in the powder compact, and the composite sample is carefully sintered at high temperature. Furthermore, this method is much simpler and more economical than the other crystal growth techniques. A capillary driving force is the main essential requirement to grow seed crystal in a polycrystalline matrix. In order to obtain high-quality crystals by the SSCG method, the grain size, density and chemical homogeneity of the polycrystalline matrix must be carefully controlled during the sintering process. In particular, the control of the matrix porosity is essential to growing non-porous, high-density crystals.

NBT single crystals were grown by flux method ^[6, 15, 27]. The solvent NaF-NaVO_3 was used. The mixture 6.5NaF:2NaVO₃:1.5NBT was placed in a platinum crucible and then

heated to a soak temperature of 1060°C, at which, during 4.5h, the dissolution took place. Afterwards this mixture was cooled at a rate 1°C/h to a temperature of 940°C at which the solvent was poured out, after that it was cooled to room temperature at 50°C/h. Transparent and light brown crystals of rectangular shape and maximal size up to 5mm were obtained.

Yellowish transparent NBT single crystals with dimensions 5x5x5 mm³ were grown using a flux technique at air atmosphere and under high-oxygen pressure atmosphere [128]. It was shown that crystals obtained under high-oxygen pressure show a lower leakage current and a better polarization switching. From neutron-scattering studies it was found [128] that the broad maximum in the electric permittivity originates in a diffusive first-order transition between the competing rhombohedral and tetragonal phases and depolarization process at T_d originates in the dynamic nature of ferroelectric regions in the interval of both phases coexistence in accordance with results presented in previous papers [16, 28, 31, 44, 61].

Czochralski method is often used to obtain crystals of perovskite structure. Crystal growth by this technique courses in the following way: a crucible with mixture is located in a furnace, and heated to a temperature slightly higher than the melting point. Next to surface of melted substance monocrystalline nucleus is drawing out. The crystal growth extends from the nucleus when temperature is decreasing. The rate of extend is equal to rate of crystal growth. The main advantage of this technique is the possibility to obtain large crystals, but the main disadvantages are a high crystallization temperature, which generates high costs and causes structural defects more probable due to the high volatility of potassium and bismuth at this temperature.

Powders of Na₂CO₃, Bi₂O₃ and TiO₂ were used as the starting reagents for obtain of NBT single crystals by the Czochralski method [5, 6]. Stoichiometric amounts were weighted and homogenized in agate vessel using alcohol during 2h. The obtained mixture was then calcined at 800°C during 4h. The crystal growth was carried out at 1350°C. The single crystals obtained with dimensions ≈1.5x1.5x2.5 cm³ were yellow-green colored.

The (1-x)NBT-xBT (0≤x≤0.14) single crystal growth by Czochralski method were obtained in similar conditions- only temperature of crystallization increased with increasing of Ba²⁺ ions content [8, 10, 93]. As expected, the Ba concentration in crystals was smaller than in solution, which indicates that the effective segregation factor is smaller than unity.

Good-quality and large-size NBT-BT single crystals with size 25-35 mm were obtained by the TSSG technique [111, 118].

Raw powders with a high-purity were used as starting reagents for obtain of 0.9NBT-0.1BT single crystal by the TSSG method [114]. The well-mixed powders were calcined

at 1000°C for 10h. Then, mixed powders with excess 20wt% of Bi_2O_3 and Na_2CO_3 as self-flux were taken in platinum crucible. Single crystals were grown with (001) oriented seed from Pt crucible. Velocities of rotation and pulling of a rod with the seed crystal were in the ranges 609 rpm and 1.2-1.5 mm/day, respectively. At the end of crystal growth, the crystal was separated from flux-melt surface and was cooled to room temperature at a rate of $50\text{-}60^\circ\text{C/h}$. A crystal with dimension $40\times 12\text{mm}$, with $d_{33}=283\text{pC/N}$, $k_t=50\%$ and $P_r=25.37\mu\text{C/cm}^2$ was obtained. These data indicate a substantial improvement of the crystal quality compared to previous results (Figs. 8-9).

Chen et al. have grown 0.94NBT-0.06BT single crystal by TSSG method with high piezoelectric properties $d_{33}=360\text{pN/C}$ and $k_t=62\%$ [115]. It was found that properties of this crystal show obvious anisotropy along its pseudocubic (001), (110) and (111) orientation.

III.6 Dielectric properties of NBT-BT single crystals around the morphotropic phase boundary

Among NBT-based systems, NBT-BT solid solutions are the most investigated ones, mainly due to the existence of a Morphotropic Phase Boundary (MPB) region (rhombohedral/tetragonal) at room temperature [129, 130].

It has been shown that in this system for a BT content equal to 6%, the boundary is a true temperature-independent MPB, the first lead-free material exhibiting such a MPB [104, 105]. In $(1-x)\text{NBT-xBT}$, for $0.05 < x < 0.11$ the structure is rhombohedral (R3m) in the unpoled state, and transformed into coexistence rhombohedral and tetragonal phase (R3c and P4mm) for $0.05 < x < 0.065$ and into R3m and P4mm for $0.065 < x < 0.11$, respectively upon poling [107, 108].

Thus, the MPB between rhombohedral and tetragonal phases in unpoled samples seems to be at $x \approx 0.11$. The domain structure of $(1-x)\text{NBT-xBT}$ ($x=0.045$ and 0.055) was examined by polarized light and piezoelectric response force microscope [104]. These studies show that the incorporation of BT to NBT: (1) refines the size of polar regions and enhances their self-organization and (2) suppresses the formation of proper ferroelastic domains at high temperatures in paraelectric phase, favoring instead the formation of improper ones that form below T_d and elastically accommodate the ferroelectric ones.

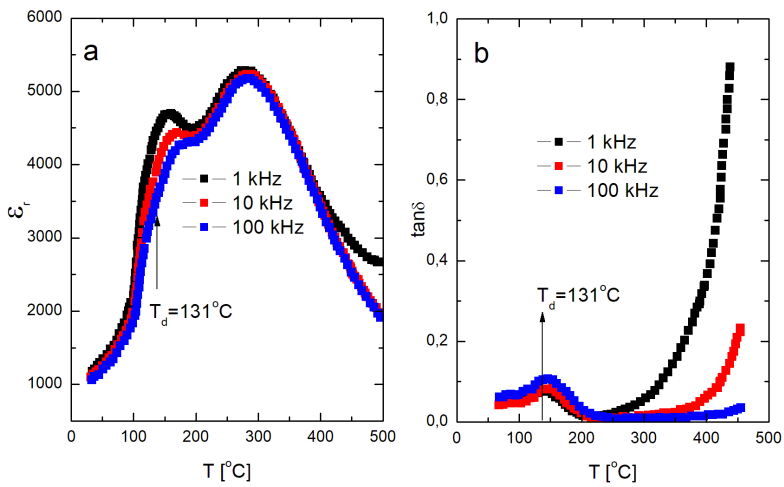


Figure 8: Dielectric properties of (001) oriented poled 0.96NBT-0.04BT crystals obtained by TSSG method as a function of temperature at the frequencies 1, 10 and 100kHz.

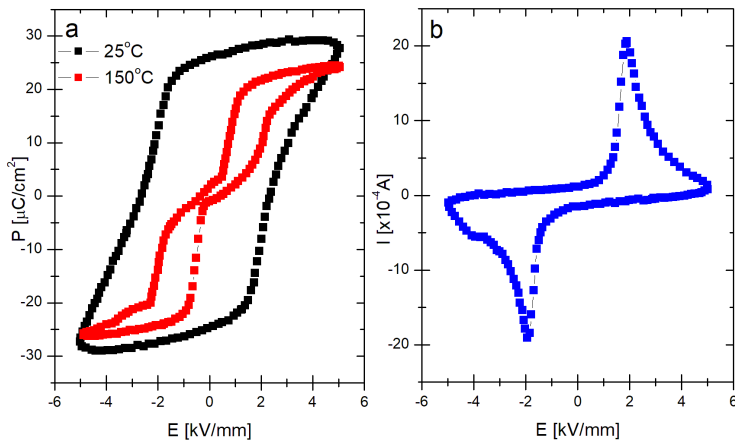


Figure 9: P–E hysteresis loop (at 25 and 150°C) and current curve (at 25°C) of (001) oriented poled 0.96NBT-0.04BT crystal obtained by TSSG method.

Chapter 6 - Properties of $\text{Na}_{0.5}\text{Bi}_{0.5}\text{TiO}_3$ and $\text{Na}_{0.5}\text{Bi}_{0.5}\text{TiO}_3$ -based single crystals

The main advantage of NBT- $\text{K}_{0.5}\text{Bi}_{0.5}\text{TiO}_3$ (NBT-KBT) system is a high depolarization temperature T_d , which may be potentially used in an extended temperature interval. In addition, this system has a rhombohedral-tetragonal MPB. However, the phase diagram of NBT-KBT and characteristics of the ferroelectric order underlying its relaxation mechanism and improved piezoelectric properties around MPB are still discussed.

The (1-x)NBT-xKBT (x=0.10, 0.16, 0.20, 0.30, 0.40, 0.50 and 0.60) single crystals with dimensions of several centimeters were grown via spontaneous nucleation from cooled molten melts (melt grown technique) under air atmosphere ^[131]. The MPB between rhombohedral and tetragonal symmetry was found at x=0.2. It was shown that a severe phase segregation during the crystallization occurred. The obtained crystals displayed clear relaxor behaviour.

The (1-x)NBT-xKBT (x=0.3 and 0.5) single crystals were grown by high-temperature self-flux, top-cooled solution growth (TCSG) and modified top seed solution growth (M-TSSG) techniques ^[132]. The crystals obtained by this method were dark brown in colour and small in size. However, the crystals obtained by TCSG and M-TSSG methods were several centimeters, with a high Curie temperature (above 350°C) and with relatively high d_{33} value (above 160pC/N). The conditions for M-TSSG method were developed based on the high-temperature phase diagram and the results of the flux growth. The NBT-KBT seed crystal obtained by the TCSG technique was introduced at the top of the solution system. A seed crystal was attached to one end of an alumina rod via PT wire, and the cooling airflow was along the alumina rod. The crystals were pulled at the rate of 0.5mm/h and rotated 10rpm.

0.65NBT-0.35KBT single crystals with tetragonal symmetry, size up to 5 mm, $P_r=10\mu\text{C}/\text{cm}^2$, $E_c=20\text{kV}/\text{cm}$, and with d_{33} value as high as 216pC/N were grown by high-temperature self-flux method ^[133].

III.7 Dielectric properties of NBT-KBT-BT single crystals

Dielectric, ferroelectric and piezoelectric properties of (1-x)NBT-xKBT (x=0.05, 0.08 and 0.12) single crystals obtained by TSSG method were presented in ^[134]. It was shown that with increasing KBT content, ferroelectrically soft behavior was created: the remnant polarization and coercive field decrease, while the piezoelectric constant and electromechanical coupling coefficient increase ($d_{33}=208$ pC/N and $k_t=53\%$ for x=0.12).

The NBT-KBT-BT single crystals grown by TSSG method exhibit enhanced

ferroelectric properties and thermal stability^[135]. Tetragonal NBT-KBT-BT single crystals show a giant strain of 0.87% along (001) direction under a low electric field of 40kV/cm^[136], and NBT-BT-NKN single crystals exhibit strain of 0.57% along (001) direction at electric field of 70kV/cm^[137]. The resulting large strain in these materials was believed to result from the reversible relaxor-ferroelectric phase transition as well as reorientation of the ferroelectric domains.

III.8 Influence of doping NBT-KBT by Mn ions

Undoped and Mn-doped 0.8NBT-0.2KBT single crystals with size up to 25mm were grown using high-temperature self-flux method^[138]. The grown crystals belong to the tetragonal symmetry and exhibit relaxor-like properties. In addition, Mn introduction to NBT leads to a decrease of electric conductivity. It was concluded that Mn acts as dilation center and generates a random field, which destroys the long-range order and leads to a relaxor-like behaviour. It was also postulated that Mn ions replace the Bi vacancies resulting in a decrease in the concentration of oxygen vacancies, which leads to the decrease in the electric conductivity.

The 0.985NBT-0.015BiZn_{0.5}Ti_{0.5}O₃ (0.985NBT-0.015BZT) single crystals with 35mm in diameter and 12mm in length, $d_{33}=121\text{pC/N}$ in (001) and a net strain up to 0.23% under 100kV/cm were grown by TSSG method^[139].

III.9 Relation between crystal structure and properties in NBT-BZT and NBT-BT

At the beginning of studies on NBT-based solid solutions and other lead-free materials with MPB, we supposed that their average/local crystal structure-properties relationship (particularly at the MPB) is similar to that observed in the well-known PZT. Unfortunately, the characteristics appearing at MPB of PZT cannot be directly transferred into lead-free materials. As we know, the nature of this relationship in NBT-based materials is extremely complicated and there is a lack of systematic theoretical and experimental examination to define this relationship.

Compounds belonging to the NBT-BT solid solution are used in the fabrication of multilayer actuators^[52, 140]. In recent papers it was suggested that NBT can be employed as an anode material for high-performing Na ion batteries^[141] and as electrocatalyst^[142]. NBT-based systems are also a potential family of peculiar electrostrictors for application in the field of actuators^[143].

IV. Some concluding remarks on NBT

Finally, we will come back to the properties of pure NBT. As mentioned earlier, numerous studies propose contradictory conclusions on number, sequence and nature of the electric order of particular phases in NBT. However, recent investigations made by advanced experimental techniques ^[144-148] do not deliver either determined results. A majority of these investigations were made on NBT in ceramic form. The obtained results indicated strong local phenomena effects on NBT properties. The role of the tilting (the anti and in-phase octahedral rotations) and off centering of TiO_6 octahedral and the $\text{Na}^+/\text{Bi}^{3+}$ ions vibration instability against octahedral and influence of lone-pairs interacting with the oxygen octahedral in phase transitions process of NBT was emphasized. Some of the mentioned discrepancies can be attributed to structure imperfections, arising from impurity of initial components and differing technologies/sintering conditions of ceramic and crystal growth, and also to a variety and complex phenomena existing in short-range scale. In addition, the properties of NBT are time-dependent. This introduces an additional uncertainty on experimental results, which is not usually taken into account. The evidence of this was described for the first time in our previous papers connected with dielectric and structural investigations of NBT ^[15, 31, 33].

V. Conclusion

The crystal growth techniques for lead-free $\text{Na}_{0.5}\text{Bi}_{0.5}\text{TiO}_3$ and $\text{Na}_{0.5}\text{Bi}_{0.5}\text{TiO}_3$ -based single crystals were presented and their properties were discussed. Apart from being environmentally-friendly, these crystals have advantages of relatively high piezoelectric constant and coupling coefficient and high mechanical strength that make them suitable for high-frequency transducers. They were successfully grown by flux technique, high-temperature self-flux technique, hydrothermal technique, top seeded solution growth technique, Czochralski and Bridgman/modified Bridgman methods.

Although, some progress in enhancing of properties of NBT-based single crystals has been made, they still exhibit some challenging properties such as large hysteresis, small operating temperature interval, high conductivity etc. in comparison with Pb-containing compounds.

Some of the above-mentioned issues should be resolved in near future by optimizing the crystal growth conditions and by using compositional/domain/defect engineering approaches, supported by poling, aging, external stress as well as annealing treatments. A decrease of the costs of single crystals growth is also needed.

This review was possible due to research carried out by numerous scientists, as evidenced by ^[148] 148 published papers in the reference list. Because of the vast number of papers connected with NBT and NBT-based materials, not all of them could be cited in the present review.

Complementary informations on authors:

jan.suchanicz@up.krakow.pl, ORCID: 0000-0003-3920-4150

kamila.kluczevska-chmielarz@up.krakow.pl, ORCID: 0000-0003-4301-7438

piotr.czaja@up.krakow.pl, ORCID: 0000-0002-8276-5706

m.nowakmalczyk@onet.pl,

marcin.was1@student.up.krakow.pl,

tkruz@meta.ua, ORCID: 0000-0002-5902-0853

Cite this paper: J. Suchanicz, K. Kluczevska-Chmielarz, P. Czaja, M. Nowakowska-Malczyk, M. Waś, T. V. Kruzina, *OAJ materials and Devices*, vol 5(1) – chap No6 in “Perovskites and other Framework Structure Crystalline Materials”, p201 (Coll. Acad. 2021) – DOI:10.23647/ca.md20202908

REFERENCES

1. A.Safari, M.Allahverdi, EK.Akdogan, *Journal of Materials Science*, **41**, 177 (2006)
2. B.Snyder, S.Lee, NB.Smith, RE.Newnham, *Journal of Materials Science*, **41**, 211 (2006)
3. K.Uchino, *Kluwer Academic Publishers, Boston, MA* (1996)
4. E.Sun, W.Cao, *Progress in Materials Science*, **65**, 124 (2014)
5. Q.Zhou, KH.Lam, H.Zheng, W.Qiu, KK.Shung, *Progress in Materials Science*, **66**, 87 (2014)
6. J.Suchanicz, J.Kwapulinski, *Ferroelectrics*, **165**, 249 (1995)
7. J.Suchanicz, *Journal of Materials Science*, **37**, 489 (2002)
8. J.Suchanicz, TV.Kruzina, *Materials Science and Engineering B*, **178**, 889-895 (2013)

Chapter 6 - Properties of Na_{0.5}Bi_{0.5}TiO₃ and Na_{0.5}Bi_{0.5}TiO₃-based single crystals

9. TV.Kruzina, VM.Duda, J.Suchanicz, *Materials Science and Engineering B*, **87**, 48 (2001)
10. J.Suchanicz, JP.Mercurio, K.Konieczny, *Ferroelectrics*, **268**, 357 (2002)
11. J.Suchanicz, M.Drulis, *Physica Status Solidi (a)*, **164**, 683 (1997)
12. J.Suchanicz, A.Jeżowski, R.Poprawski, S.Dacko, *Physica Status Solidi (b)*, **221**, 789 (2000)
13. M.Drulis, J.Suchanicz, *Physica Status Solidi (a)*, **177**, 367 (2000)
14. J.Suchanicz, TV.Kruzina, *Ferroelectrics*, **317**, 109 (2005)
15. J.Suchanicz, K.Roleder, J.Kwapuliński, I.Jankowska – Sumara, *Phase Transitions*, **57**, 173 (1996)
16. J.Suchanicz, *Materials Science and Engineering B*, **55**, 114 (1998)
17. J.Suchanicz, B.Glos, G.Stopa, TV.Kruzina, J.Kusz, M.Zubko, W.Hofmeister, I.Jankowska-Sumara, D.Wcisło, K.Konieczny, R.Rosiek, A.Finder, K.Pytel, M.Dambekalne, A.Sternberg, *Integrated Ferroelectrics*, **108**, 98 (2009)
18. JA.Zvirgzds, PP.Kapostins, JV.Zvirgzde, TV.Kruzina, *Ferroelectrics*, **40**, 75 (1982)
19. VA.Shuvaeva, D.Zekira, AM.Glazer, Q.Jiang, SM.Weber, P.Bhattacharya, PA.Thomas, *Physical Review B*, **71**, 174114 (1-8) (2005)
20. GA.Smolenskii, VA.Isupov, AI.Aganovskaya, SN.Popov, *Fizika Tverdogo Tela*, **2**, 2906 (1960) (in Russian)
21. VV.Ivanova, AG.Kapyshev, YN.Venevtsev, GS.Zhdanov, *Izvestiya Akademii Nauk SSSR*, **26**, 354–356 (1962) (in Russian)
22. K.Sakata, Y.Masuda, *Ferroelectrics*, **7**, 347 (1974)
23. IP.Pronin, PP.Syrnikov, VA.Isupov, GA.Smolensky, *Pisma v Zhurnal Tekhnicheskoi Fiziki*, **5**, 705 (1979) (in Russian)
24. IP.Pronin, PP.Syrnikov, VA.Isupov, VM.Egorov, NV.Zaitseva, *Ferroelectrics*, **25**, 395 (1980)
25. IP.Pronin, PP.Syrnikov, VA.Isupov, GA.Smolensky, *Pisma v Zhurnal Tekhnicheskoi Fiziki*, **8**, 1809 (1982) (in Russian)
26. SM.Emelyanov, IP.Raeyvsky, VG.Smotrakov, FI.Savenko, *Fizika Tverdogo Tela*, **26**, 1897 (1984) (in Russian)
27. SM.Emelyanov, IP.Raeyvsky, VG.Smotrakov, FI.Savenko, *Neorganicheskiye materialy*, **21**, 839 (1985) (in Russian)
28. J.Suchanicz, K.Roleder, A.Kania, J.Handerek, *Ferroelectrics*, **77**, 107 (1988)
29. VP.Avramenko, TV.Kruzina, AYu.Kudzin, GCH.Sokolyansky, AS.Yudin, *Fizika Tverdogo Tela*, **31**, 325 (1989) (in Russian)
30. VP.Avramenko, TV.Kruzina, AYu.Kudzin, GCH.Sokolyansky, *Ferroelectrics*, **174**, 71 (1995)
31. K.Roleder, J.Suchanicz, A.Kania, *Ferroelectrics*, **89**, 1 (1989)
32. J.Suchanicz, WS.Ptak, *Ferroelectrics Letters*, **12**, 71 (1990)
33. J.Suchanicz, *Ferroelectrics*, **200**, 319 (1997)

34. J.Suchanicz, WS.Ptak, *Izvestiya Akademii Nauk SSSR Seriya Fizicheskaya*, **55**, 555 (1991)
35. VA.Isupov, IP.Pronin, TV.Kruzina, *Ferroelectrics Letters*, **2**, 205 (1984)
36. IG.Siny, TA.Smirnova, TV.Kruzina, *Fizika Tverdogo Tela*, **33**, 110 (1991) (in Russian)
37. SG.Lushnikov, SN.Gvasaliya, IG.Siny, IL.Sashin, VH.Schmidt, Y.Uesu, *Solid State Communications*, **116**, 41 (2000)
38. YN.Xu, WY.Ching, *Philosophical Magazine*, **B80**, 1141 (2000)
39. M.Zeng, SW.Or, HLW.Chan, *Journal of Applied Physics*, **107**, 043513 (2010)
40. SE.Park, SJ.Chung, IT.Kim, KS.Hong, *Journal of the American Ceramic Society*, **77**, 2611 (1994)
41. SE.Park, SJ.Chung, IT.Kim, *Journal of the American Ceramic Society*, **79**, 1290 (1996)
42. J.Kusz, J.Suchanicz, H.Böhm, J.Warczewski, *Phase Transitions*, **70**, 223 (1999)
43. KC.Meyer, L.Koch, K.Albe, *Journal of the American Ceramic Society*, **101**, 472 (2017)
44. SB.Vakhrushev, VA.Isupov, BE.Kvyatkovsky, NM.Okuneva, IP.Pronin, GA.Smolensky, PP.Syrnikov, *Ferroelectrics*, **63**, 153 (1985)
45. GO.Jones, PA.Thomas, *Acta Crystallographica B*, **58**, 168 (2002)
46. J.Suchanicz, K.Kluczevska, P.Czaja, A.Kania, K.Konieczny, B.Handke, M.Sokolowski, MP.Trubitsyn, TV.Kruzina, *Ceramics International*, **43**, 17194 (2017)
47. V.Dorcet, G.Troilliarnd, P.Boullay, *Chemistry of Materials*, **20**, 5061 (2008)
48. S.Gorfman, PA.Thomas, *Journal of Applied Crystallography*, **43**, 1409 (2010)
49. E.Aksel, JS.Forrester, JL.Jones, PA.Thomas, K.Page, MR.Suchomel, *Applied Physics Letters*, **98**, 152901 (2011)
50. BN.Rao, AN.Fitch, R.Ranjan, *Physical Review B*, **87**, 060102 (R) (2013)
51. AM.Balagurov, EY.Koroleva, AA.Naberezhnov, VP.Sakhnenhoo, BN.Savrnk, AA.Ter-Oganessian, SB.Vakhrushev, *Phase Transitions*, **79**, 163 (2006)
52. K.Reichmann, A.Feteira, M.Li, *Materials*, **8**, 8467 (2015)
53. J.Suchanicz, R.Poprawski, S.Matyjasik, *Ferroelectrics*, **192**, 329 (1997)
54. SB.Vakhrushev, BE.Kviatkovsky, NM.Okuneva, EL.Placenoa, LP.Syrnikov, *Pisma v Zhurnal Tekhnicheskoi Fiziki*, **35**, 111 (1982)
55. SB.Vakhrushev, BG.Ivanicky, BE.Kvyatkovsky, AN.Maistrienko, RS.Malysheva, NM.Okunieva, NN.Parfienova, *Fizika Tverdogo Tela*, **25**, 2613-2616, (1983) (in Russian)
56. SB.Vakhrushev, BE.Kviatkovsky, NN.Okunieva, EL.Plachenova, PP.Syrnikov, *Fizika Tverdogo Tela*, **25**, 2529 -2531 (1983) (in Russian)
57. SB.Vakhrushev, BE.Kvyatkovsky, RS.Malysheva, NN.Okuneva, PP.Syrnikov, *Kristallografiya*, **1**, 154 (1989) (in Russian)
58. SB.Vakhrushev, BE.Kviatkovsky, NM.Okuneva, EL.Placenoa, LP.Syrnikov, *Pisma*

Chapter 6 - Properties of $\text{Na}_{0.5}\text{Bi}_{0.5}\text{TiO}_3$ and $\text{Na}_{0.5}\text{Bi}_{0.5}\text{TiO}_3$ -based single crystals

- v Zhurnal Tekhnicheskoi Fiziki*, **35**, 111 (1982)
59. IP.Aleksandrova, JN.Ivanova, AA.Suchovsky, SB.Vakhrushev, *Fizika Tverdogo Tela*, **48**, 1056 (2006)
 60. IP.Aleksandrova, AA.Suchovsky, YuN.Ivanov, YuE.Yablonskaya, SB.Vakhrushev, *Ferroelectrics*, **378**, 16 (2009)
 61. J.Suchanicz, *Ferroelectrics*, **209**, 561 (1998)
 62. A.Molak, J.Suchanicz, *Ferroelectrics*, **189**, 53-59 (1996)
 63. J.Suchanicz, D.Sitko, N-TH.Kim-Ngan, AG.Balogh, *Journal of Applied Physics*, **104**, 0941106 (1-4) (2008)
 64. I.Faszczowy, J.Suchanicz, TV.Kruzina, T.Maslanka, M.Ingwer-Zabowska, W.Piekarczyk, B.Handke, P.Jelen, M.Sokolowski, *Ferroelectrics*, **461**, 101-106 (2014)
 65. VA.Isupov, TV.Kruzina, *Izvestiya Akademii Nauk SSSR Seriya Fizicheskaya*, **48**, 1178 (1984) (in Russian)
 66. TV.Kruzina, SP.Reprinceva, *Izvestiya Akademii Nauk SSSR Seriya Fizicheskaya*, **53**, 1327 (1989) (in Russian)
 67. J.Suchanicz, *Journal of Physics and Chemistry of Solids*, **62**, 1271 (2000)
 68. TV.Kruzina, VM.Sidak, MP.Trubitsyn, SA.Popov, J.Suchanicz, *Ferroelectrics*, **462**, 140 (2014)
 69. TV.Kruzina, VM.Sidak, MP.Trubitsyn, SA.Popov, AYu.Tuluk, J.Suchanicz, *Acta Physica Polonica A*, **133**, 816 (2018)
 70. J.Yao, W.Ge, L.Yan, L.Luo, J.Li, D.Viehland, H.Luo, *Applied Physics Letters*, **96**, 222905 (2010)
 71. J.Yao, W.Ge, Y.Yang, L.Luo, J.Li, D.Viehland, S.Bhatatacharyya, Q.Zhang, H.Luo, *Journal of Applied Physics*, **108**, 064114 (2010)
 72. P.Ramesh Babu, R.Selvamani, G.Singh, S.Kalainathan, R.Babu, VS.Tiwari, *Journal of Alloys and Compounds*, **721**, 199 (2017)
 73. J.Petzelt, S.Kamba, J.Fabry, D.Noujni, V.Porokhonsky, A.Pashkin, I.Franke, K.Roleder, J.Suchanicz, R.Klein, GE.Kugel, *Journal of Physics: Condensed Matter*, **16**, 2719 (2004)
 74. B.Andriyevsky, J.Suchanicz, Ch.Cobet, A.Patryn, N.Esser, B.Kosturek, *Phase Transitions*, **82**, 567-575 (2009)
 75. MS.Zhang, JF.Scott, JA.Zvirgds, *Ferroelectrics Letters*, **6**, 147 (1986)
 76. IG.Siny, TA.Smirnova, TV.Kruzina, *Ferroelectrics*, **124**, 207 (1991)
 77. IG.Siny, E.Husson, JM.Beny, SG.Lushnikov, EA.Rogacheva, PP.Syrnikov, *Ferroelectrics*, **248**, 57 (2000)
 78. J.Kreisel, A.M.Glazer, G.Jones, PA.Thomas, L.Abello, G.Lucazeau, *Journal of Physics: Condensed Matter*, **12**, 3267 (2000)
 79. MK.Niranjan, T.Karthik, S.Asthana, J.Pan, UV.Waghmare, *Journal of Applied Physics*, **113**, 194106 (2013)
 80. J.Kreisel, P.Bouvier, *Journal of Raman Spectroscopy*, **34**, 524 (2003)

81. J.Kreisel, AM.Glazer, P.Bouvier, G.Lucazeau, *Physical Review B*, **63**, 174106 (2001)
82. BN.Rao, R.Datta, SS.Chandrashekarm, DK.Mishra, V.Sathe, A.Senyshyn, R.Ranjan, *Physical Review B*, **88**, 224103 (2013)
83. BK.Barick, KK.Mishra, AK.Arora, RNP.Choudhary, DK.Pradhan, *Journal of Physics D: Applied Physics*, **44**, 355402 (2011)
84. J.Suchanicz, D.Sitko, Š.Svirskas, M.Ivanov, A.Kežionis, J.Banys, P.Czaja, TV.Kruzina, J.Szczęśny, *Ferroelectrics*, **532**, 38 (2018)
85. BP.Burton, E.Cockayne, *The 11th williamsburg workshop on fundamental physics of ferroelectrics. AIP Conference Proceedings*, **582**, 82 (2001)
86. M.Gröting, S.Hayn, K.Albe, *Journal of Solid State Chemistry*, **184**, 2041 (2011)
87. KC.Meyer, M.Gröting, S.Hayn, K.Albe, *Journal of Solid State Chemistry*, **227**, 117 (2015)
88. KC.Meyer, K.Albe, *J.Mat.Chem.*, **A5**, 4368 (2017)
89. H.Lü, S.Wang, X.Wang, *Journal of Applied Physics*, **115**, 124107 (2014)
90. X.Ren, *Nature*, **3**, 91 (2004)
91. J.Suchanicz, K.Świerczek, E.Nogas-Ćwikiel, K.Konieczny, D.Sitko, *Journal of the European Ceramic Society*, **35**, 1777 (2015)
92. AM.Antonenko, AYu.Kudzin, MG.Gavsin, *Fizika Tverdogo Tela*, **39**, 920 (1997) (in Russian)
93. J.Suchanicz, TV.Kruzina, VG.Pozdeev, SA.Popov, *Phase Transitions*, **89**, 310 (2016)
94. J.Suchanicz, B.Glos, G.Stopa, TV.Kruzina, J.Kusz, M.Zubko, W.Hofmeister, I.Jankowska-Sumara, D.Wcisło, K.Konieczny, R.Rosiek, A.Finder, K.Pytel, M.Dambekalne, A.Sternberg, *Integrated Ferroelectrics*, **108**, 98 (2009)
95. YM.Chiang, GW.Farrey, AN.Soukhojak, *Applied Physics Letters*, **73**, 3683 (1998)
96. YM.Chiang, GW.Farrey, AN.Soukhojak, SA.Sheets, *Proc.9 US-Japan Seminar on Dielectric and piezoelectric Ceramics*, Nov. 3-5 (1999), Okinawa, Japan
97. AN.Soukhojak, H.Wang, GW.Farrey, YM.Chiang, *Journal of Physics and Chemistry of Solids*, **61**, 301 (2000)
98. Y.Hosono, K.Harada, Y.Yamashita, *Japanese Journal of Applied Physics*, **40**, 5722 (2001)
99. MG.Gavshin, VI.Pastukhov, *Ferroelectrics*, **205**, 81 (1998)
100. E.Dulkin, J.Suchanicz, A.Kania, M.Roth, *Materials Research*, **21**, e20170953 (2018)
101. J.Bubesh Babu, G.Madeswaran, H.Ming, DF.Zhang, XL.Chen, R.Dhanasekaran, *Journal of Crystal Growth*, **310**, 467 (2008)
102. Q.Zhang, X.Zhao, R.Sun, H.Luo, *Physica Status Solidi (a)*, **208**, 1012 (2011)
103. L.Zheng, X.Yi, S.Zhang, W.Jiang, B.Yang, R.Zhang, W.Cao, *Applied Physics Letters*, **103**, 122905 (2013)
104. J.Yao, L.Yan, W.Ge, L.Luo, J.Li, D.Viehland, Q.Zhang, H.Luo, *Physical Review*

Chapter 6 - Properties of Na_{0.5}Bi_{0.5}TiO₃ and Na_{0.5}Bi_{0.5}TiO₃-based single crystals

- B*, **83**, 054107 (2011)
105. B.Wylie-van Eerd, D.Damjanovic, N.Klein, N.Setter, J.Trodahl, *Physical Review B*, **82**, 104112 (2011)
 106. T.Takenaka, M.Maruyama, K.Sakata, *Japanese Journal of Applied Physics*, **30(B)**, 2236 (1991)
 107. W.Jo, JE.Daniels, JL.Jones, X.Tan, PA.Thomas, D.Damjanovic, J.Rödel, *Journal of Applied Physics*, **109**, 014110 (2011)
 108. R.Garg, BN.Rao, A.Senyszyn, PSR.Krishna, R.Ranjan, *Physical Review B*, **88**, 014103 (2013)
 109. J.Yao, N.Monsegue, M.Murayama, W.Leng, *Applied Physics Letters*, **100**, 012901 (2012)
 110. F.Craciun, C.Galassi, R.Birjega, *Journal of Applied Physics*, **112**, 124106 (2012)
 111. D.Schneider, W.Jo, D.Rytz, T.Granzow, *Journal of Applied Physics*, **116**, 044111 (2014)
 112. D.Schneider, J.Rödel, D.Rytz, T.Granzow, *Journal of the American Ceramic Society*, **98**, 3966 (2015)
 113. Q.Zhang, Y.Zhang, F.Wang, Y.Wang, D.Lin, X.Zhao, H.Luo, W.Ge, D.Viehland, *Applied Physics Letters*, **95**, 102904 (2009)
 114. Q.Zhang, Y.Zhang, F.Wang, Y.Wang, D.Lin, X.Li, X.Zhao, H.Luo, *Journal of Crystal Growth*, **312**, 457 (2010)
 115. CS.Chen, CS.Tu, PY.Chen, Y.Ting, SJ.Chiu, CM.Hung, HY.Lee, SF.Wang, J.Anthoninappen, VH.Schmidt, RR.Chien, *Journal of Crystal Growth*, **393**, 129-133 (2014)
 116. L.Zheng, X.Yi, S.Zhang, W.Jiang, B.Yang, R.Zhang, W.Cao, *Applied Physics Letters*, **103**, 122905-1 – 122905-4 (2013)
 117. C.Chen, H.Zhang, H.Deng, T.Huang, X.Li, X.Zhao, Z.Hu, D.Wang, H.Luo, *Applied Physics Letters*, **104**, 142902 (2014)
 118. C.Chen, X.Jiang, Y.Li, F.Wang, Q.Zhang, H.Luo, *Journal of Applied Physics*, **108**, 124106 (2010)
 119. J.Zhu, J.Zhang, K.Jiang, H.Zhang, Z.Hu, H.Luo, J.Chu, *Journal of the American Ceramic Society*, **99**, 2408 (2016)
 120. L.Luo, W.Ge, J.Li, D.Viehland, C.Farley, R.Bodnar, Q.Zhang, H.Luo, *Journal of Applied Physics*, **109**, 113507 (2011)
 121. KS.Moon, D.Rout, HY.Lee, SJ.Kang, *Journal of Crystal Growth*, **317**, 28 (2011)
 122. WW.Ge, JF.Li, D.Viehland, HS.Luo, *Journal of the American Ceramic Society*, **93**, 1372 (2010)
 123. W.Ge, H.Liu, X.Zhao, W.Zhong, X.Pan, T.He, D.Lin, H.Xu, X.Jiang, H.Luo, *Journal of Alloys and Compounds*, **462**, 256 (2008)
 124. Q.Zhang, X.Li, R.Sun, X.Wu, B.Ren, X.Zhao, H.Luo, *Journal of Crystal Growth*, **318**, 870 (2011)

125. J.Yao, Y.Yang, N.Monsegue, Y.Li, J.Li, Q.Zhang, W.Ge, H.Luo, D.Viehland, *Applied Physics Letters*, **98**, 132903 (2011)
126. PW.Rehrig, WS.Hackenberger, X.Jiang, TR.Shrouf, S.Zhang, R.Speyer, *IEEE Ultrasonics Symposium-769* (2003)
127. S.Zhang, F.Li, *Journal of Applied Physics*, **111**, 031301 (2012)
128. M.Matsuura, H.Iida, K.Ohwada, Y.Noguchi, M.Miyayama, *Physical Review B*, **87**, 064109 (2013)
129. RR.McQuade, MR.Dolgo, *Journal of Solid State Chemistry*, **242**, 140 (2016)
130. J.Suchanicz, I.Jankowska-Sumara, TV.Kruzina, *Journal of Electroceramics*, **27**, 45 (2011)
131. H.Hie, L.Jin, D.Shen, X.Wang, G.Shen, *Journal of Crystal Growth*, **311**, 3626 (2009)
132. X.Yi, H.Chen, W.Cao, M.Zhao, D.Yang, G.Ma, C.Yang, J.Han, *Journal of Crystal Growth*, **281**, 364 (2005)
133. S.Bhandari, N.Sinha, G.Ray, B.Kumar, *CrystEngComm*, **16**, 4459 (2014)
134. H.Zhang, C.Chen, X.Zhao, H.Deng, B.Ren, X.Li, H.Luo, S.Li, *Solid State Communications*, **201**, 125 (2015)
135. H.Yan, H.Zhang, H.Deng, X.Liu, X.Zhao, D.Lin, X.Li, H.Luo, J-H.Ko, CW.Ahn, *Scripta Materialia*, **113**, 43 (2016)
136. S.Terenishi, M.Suzuki, Y.Noguchi, M.Miyayama, C.Moriyoshi, Y.Kuroiwa, K.Tawa, S.Mori, *Applied Physics Letters*, **92**, 182905 (2008)
137. J-H.Park, H-Y.Lee, S-JL.Kang, *Applied Physics Letters*, **104**, 222910 (2014)
138. GA.Babu, R.Subramaniyan, RI.Bhaumik, S.Ganesamoorthy, P.Ramasamy, PK.Gupta, *Materials Research Bulletin*, **53**, 136 (2014)
139. C.Chen, HW.Zhang, XY.Zhao, H.Deng, XB.Li, HS.Luo, *Journal of the American Ceramic Society*, **97**, 1 (2014)
140. W.Krauss, D.Schütz, D.Naderer Orosel, K.Reichmann, *Journal of the European Ceramic Society*, **31**, 1857 (2011)
141. KK.Bharathi, B.Moorthy, HK.Dara, L.Durai, *Journal of Materials Science*, **54**, 13236 (2019)
142. HS.Kushwaha, A.Halder, R.Vaish, *Journal of Materials Science*, **53**, 1414 (2018)
143. J.Yin, G.Liu, C.Zhao, Y.Huang, Z.Li, X.Zhang, K.Wang, J.Wu, *Journal of Materials Chemistry A*, **7**, 13658 (2019)
144. TM.Usher, I.Levin, JE.Daniels, JL.Jones, *Scientific Reports*, **5**, 14678 (2015)
145. G.Deng, S.Danilkin, H.Zhang, P.Imperia, X.Li, X.Zhao, H.Luo, *Physical Review B*, **90**, 134104 (2014)
146. R.Beanland, PA.Thomas, *Physical Review B*, **89**, 174102 (2014)
147. D.Shütz, M.Deluca, W.Krauss, A.Feteira, T.Jackson, K.Reichmann, *Advanced Functional Materials*, **22**, 2285-2294 (2012)
148. BN.Rao, L.Olivi, V.Sathe, R.Ranjan, *Physical Review B*, **93**, 024106 (2016)